UDC: 538.9 Condensed matter Physics, Solid state Physics, Theoretical Condensed matter Physics

SIMPLE CUBIC FERROMAGNETIC FILMS WITH THREE LAYERS AS DESCRIBED BY THIRD ORDER PERTURBED HAMILTONIAN

P. Samarasekara[1, 3] and N.U.S. Yapa[2, 3]

[1]Department of Physics, University of Peradeniya, Peradeniya, Sri Lanka
[2]Department of Physics, Open University of Sri Lanka, Kandy, Sri Lanka
[3]Postgraduate Institute of Science, University of Peradeniya, Sri Lanka.

Abstract
Third order perturbed Heisenberg Hamiltonian was employed to find the energy of simple cubic ferromagnetic ultra-thin films with three layers. All the magnetic energy parameters such as spin exchange interaction, magnetic dipole interaction, second order magnetic anisotropy, fourth order magnetic anisotropy, applied magnetic field, demagnetization factor and stress induced anisotropy were included in the third order perturbed Heisenberg Hamiltonian. 3-D plots of stress induced anisotropy, out of plane magnetic field, demagnetization factor and spin exchange interaction are presented in this manuscript. Magnetic easy and hard directions were determined using these 3-D plots.
Keywords: Spin, Third order perturbation, Heisenberg Hamiltonian, ferromagnetic thin films

1. Introduction:

Ferromagnetic films have been described using many different theoretical models. EuTe films with surface elastic stresses have been theoretically investigated using Heisenberg Hamiltonian [1]. Magnetostriction of dc magnetron sputtered FeTaN thin films has been theoretically explained using the theory of De Vries [2]. Magnetic layers of Ni on Cu have been theoretically studied using the Korringa-Kohn-Rostoker Green's function method [3]. Electric and magnetic properties of multiferroic thin films have been theoretically investigated by modified Heisenberg and transverse Ising model using Green's function technique [4]. The quasistatic magnetic hysteresis of ferromagnetic thin films grown on a vicinal substrate has been theoretically described by Monte Carlo simulations within a 2D model [5]. Structural and magnetic properties of two dimensional FeCo orders alloys deposited on W(110) substrates have been investigated using first principles band structure theory [6].

Heisenberg Hamiltonian was employed to solve the problems of magnetic thin films as summarized below. Ferromagnetic thin films have been previously studied using the Heisenberg Hamiltonian with spin exchange interaction, magnetic dipole interaction, applied magnetic field, second and fourth order magnetic anisotropy [7, 8, 9]. Magnetization reversal and domain structure in thin magnetic films have been theoretically investigated [10]. In-plane dipole coupling anisotropy of a square ferromagnetic Heisenberg monolayer has been described using Heisenberg Hamiltonian [11]. Effect of the interracial coupling on the magnetic ordering in ferro-antiferromagntic bilayers has been studied using Heisenberg Hamiltonian [12].

Previously strontium ferrite [13] and nickel ferrite [14] films were synthesized using sputtering by us. In addition, lithium mixed ferrite films were fabricated using pulsed laser deposition [15]. For all these films, the coercivity of film increased due to the stress induced anisotropy. The change of coercivity due to the stress induced anisotropy was qualitatively calculated for all these films. The calculated values of the change of coercivity agreed with the

experimentally found values. So the stress induced anisotropy plays a major role in magnetic thin fabrications. Previously the Heisenberg Hamiltonian was employed to investigate the second order perturbed energy of ultrathin ferromagnetic films [16], thick ferromagnetic films [17], unperturbed energy of spinel ferrite films [18], second order perturbed energy of thick ferromagnetic films [19], third order perturbed energy of thick spinel ferrite [20], third order perturbed energy of thin spinel ferrite [21], second order perturbed energy of spinel ferrite [22] and spin reorientation of barium ferrite [23].

2. Model:
Modified classical Heisenberg Hamiltonian with all the magnetic parameters is given as below.

$$
\begin{aligned}
H= &-\frac{J}{2}\sum_{m,n}\vec{S}_m.\vec{S}_n + \frac{\omega}{2}\sum_{m\neq n}(\frac{\vec{S}_m.\vec{S}_n}{r_{mn}^{\,3}} - \frac{3(\vec{S}_m.\vec{r}_{mn})(\vec{r}_{mn}.\vec{S}_n)}{r_{mn}^{\,5}}) - \sum_m D_{\lambda_m}^{\,(2)}(S_m^{\,z})^2 - \sum_m D_{\lambda_m}^{\,(4)}(S_m^{\,z})^4 \\
&-\sum_{m,n}[\vec{H}-(N_d\vec{S}_n/\mu_0)].\vec{S}_m - \sum_m K_s Sin 2\theta_m
\end{aligned} \tag{1}
$$

Here J is spin exchange interaction, ω is the strength of long range dipole interaction, θ is azimuthal angle of spin, $D_m^{(2)}$ and $D_m^{(4)}$ are second and fourth order anisotropy constants, H_{in} and H_{out} are in plane and out of plane applied magnetic fields, K_s is stress induced anisotropy constant, n and m are spin plane indices, and N is total number of layers in film. When the stress applies normal to the film plane, the angle between m[th] spin and the stress is θ_m. Because the size of the unit cell of ferromagnetic structure is taken as one, r_{mn} is taken as a fraction of the size of the unit cell of ferromagnetic structure.

The total energy per unit spin can be deduced to the following equation.

$$
\begin{aligned}
E(\theta)= &-\frac{1}{2}\sum_{m,n=1}^{N}[(JZ_{|m-n|} - \frac{\omega}{4}\Phi_{|m-n|})\cos(\theta_m-\theta_n) - \frac{3\omega}{4}\Phi_{|m-n|}\cos(\theta_m+\theta_n)] \\
&-\sum_{m=1}^{N}(D_m^{(2)}\cos^2\theta_m + D_m^{(4)}\cos^4\theta_m + H_{in}\sin\theta_m + H_{out}\cos\theta_m) \\
&+\sum_{m,n=1}^{N}\frac{N_d}{\mu_0}\cos(\theta_m-\theta_n) - K_s\sum_{m=1}^{N}\sin 2\theta_m
\end{aligned} \tag{2}
$$

where m (or n) $Z_{|m-n|}, \phi_{|m-n|}, \theta_m(or\,\theta_n)$, N, H_{in} and H_{out} being indices of layers, number of nearest spin neighbors, constant arising from summation of dipole interactions, azimuthal angles of spins, total number of layers, in plane applied field and out of plane applied field, respectively.

With some perturbation, above angles θ_m and θ_n measured with film normal can be expressed in forms of $\theta_m=\theta+\varepsilon_m$ and $\theta_n=\theta+\varepsilon_n$, and above energy can be expanded up to the third order of ε as following. Here ε_m (or ε_n) is a small perturbation of the angle.

$$
E(\theta)=E_0+E(\varepsilon)+E(\varepsilon^2)+E(\varepsilon^3) \tag{3}
$$

Here $E_0= -\frac{1}{2}\sum_{m,n=1}^{N}(JZ_{|m-n|} - \frac{\omega}{4}\Phi_{|m-n|}) + \frac{3\omega}{8}\cos 2\theta\sum_{m,n=1}^{N}\Phi_{|m-n|}$

$$
-\cos^2\theta\sum_{m=1}^{N}D_m^{(2)} - \cos^4\theta\sum_{m=1}^{N}D_m^{(4)} - N(H_{in}\sin\theta + H_{out}\cos\theta - \frac{N_d}{\mu_0} + K_s\sin 2\theta)
$$

$$
E(\varepsilon)= -\frac{3\omega}{8}\sin 2\theta\sum_{m,n=1}^{N}\Phi_{|m-n|}(\varepsilon_m+\varepsilon_n) + \sin 2\theta\sum_{m=1}^{N}D_m^{(2)}\varepsilon_m + 2\cos^2\theta\sin 2\theta\sum_{m=1}^{N}D_m^{(4)}\varepsilon_m
$$

$$- H_{in} \cos\theta \sum_{m=1}^{N} \varepsilon_m + H_{out} \sin\theta \sum_{m=1}^{N} \varepsilon_m - 2K_s \cos 2\theta \sum_{m=1}^{N} \varepsilon_m$$

$$\mathrm{E}\,(\varepsilon^2) = \frac{1}{4} \sum_{m,n=1}^{N} (JZ_{|m-n|} - \frac{\omega}{4}\Phi_{|m-n|})(\varepsilon_m - \varepsilon_n)^2 - \frac{3\omega}{16}\cos 2\theta \sum_{m,n=1}^{N} \Phi_{|m-n|}(\varepsilon_m + \varepsilon_n)^2$$

$$- (\sin^2\theta - \cos^2\theta)\sum_{m=1}^{N} D_m^{(2)} \varepsilon_m^{\ 2} + 2\cos^2\theta(\cos^2\theta - 3\sin^2\theta)\sum_{m=1}^{N} D_m^{(4)} \varepsilon_m^{\ 2}$$

$$+ \frac{H_{in}}{2}\sin\theta \sum_{m=1}^{N} \varepsilon_m^{\ 2} + \frac{H_{out}}{2}\cos\theta \sum_{m=1}^{N} \varepsilon_m^{\ 2} - \frac{N_d}{2\mu_0}\sum_{m,n=1}^{N}(\varepsilon_m - \varepsilon_n)^2$$

$$+ 2K_s \sin 2\theta \sum_{m=1}^{N} \varepsilon_m^{\ 2}$$

$$E(\varepsilon^3) = \frac{\omega}{16}\sin 2\theta \sum_{m,n=1}^{N}(\varepsilon_m + \varepsilon_n)^3 \phi_{|m-n|} - \frac{4}{3}\cos\theta \sin\theta \sum_{m=1}^{N} D_m^{(2)} \varepsilon_m^{\ 3}$$

$$- 4\cos\theta \sin\theta(\frac{5}{3}\cos^2\theta - \sin^2\theta)\sum_{m=1}^{N} D_m^{(4)} \varepsilon_m^{\ 3} + \frac{H_{in}}{6}\cos\theta \sum_{m=1}^{N} \varepsilon_m^{\ 3}$$

$$- \frac{H_{out}}{6}\sin\theta \sum_{m=1}^{N} \varepsilon_m^{\ 3} + \frac{4K_s}{3}\cos 2\theta \sum_{m=1}^{N} \varepsilon_m^{\ 3} \tag{4}$$

After using the constraint $\sum_{m=1}^{N} \varepsilon_m = 0$, $\mathrm{E}(\varepsilon) = \vec{\alpha}.\vec{\varepsilon}$

Here $\vec{\alpha}(\varepsilon) = \vec{B}(\theta)\sin 2\theta$ are the terms of matrices with

$$B_\lambda(\theta) = -\frac{3\omega}{4}\sum_{m=1}^{N} \Phi_{|\lambda-m|} + D_\lambda^{(2)} + 2D_\lambda^{(4)}\cos^2\theta \tag{5}$$

Also $E(\varepsilon^2) = \frac{1}{2}\vec{\varepsilon}.C.\vec{\varepsilon} \tag{6}$

Here the elements of matrix C can be given as following,

$$C_{mn} = -(JZ_{|m-n|} - \frac{\omega}{4}\Phi_{|m-n|}) - \frac{3\omega}{4}\cos 2\theta\Phi_{|m-n|} + \frac{2N_d}{\mu_0}$$

$$+ \delta_{mn}\{\sum_{\lambda=1}^{N}[JZ_{|m-\lambda|} - \Phi_{|m-\lambda|}(\frac{\omega}{4} + \frac{3\omega}{4}\cos 2\theta)] - 2(\sin^2\theta - \cos^2\theta)D_m^{(2)}$$

$$+ 4\cos^2\theta(\cos^2\theta - 3\sin^2\theta)D_m^{(4)} + H_{in}\sin\theta + H_{out}\cos\theta - \frac{4N_d}{\mu_0} + 4K_s \sin 2\theta\} \tag{7}$$

In addition, third order can be expressed as the

$$E(\varepsilon^3) = \varepsilon^2 \beta.\vec{\varepsilon} \tag{8}$$

Here elements of matrix β can be given as following,

$$\beta_{mn} = \frac{3\omega}{8}\sin 2\theta\Phi_{|m-n|} + \delta_{mn}\{\frac{\omega}{8}\sin 2\theta[A_m - \Phi_0] - \frac{4}{3}\cos\theta \sin\theta D_m^{(2)}$$

$$- 4\cos\theta \sin\theta(\frac{5}{3}\cos^2\theta - \sin^2\theta)D_m^{(4)} + \frac{H_{in}}{6}\cos\theta - \frac{H_{out}}{6}\sin\theta$$

$$+ \frac{4K_s}{3}\cos 2\theta\}$$

Also $\beta_{nm}=\beta_{mn}$, implying that matrix β is symmetric.
After substituting equations (8) and (6) in equation (3), total energy can be expressed as

$$E(\theta)=E_0+ \vec{\alpha}.\vec{\varepsilon} +\frac{1}{2}\vec{\varepsilon}.C.\vec{\varepsilon} + \varepsilon^2 \beta.\vec{\varepsilon}$$

At the energetically favorable state, the derivative of above $E(\theta)$ with respect to ε will be zero. Using that condition, ε can be found. After substituting that ε in above equation of $E(\theta)$, following equation can be derived.

$$E(\theta)=E_0 - \frac{1}{2}\vec{\alpha}.C^+.\vec{\alpha} - (C^+\alpha)^2 \vec{\beta}(C^+\alpha)$$

The total magnetic energy have been calculated only for three layers (N=3), and the equation have been proved under the assumption of $D_1^{(2)}=D_2^{(2)} =D_3^{(2)}$ and $D_1^{(4)}=D_2^{(4)}=D_3^{(4)}$.
Following equation has been used to calculate the elements of matrix C^+.

$$C.C^+ =1-\frac{E}{N}$$

Each element of matrix E is one, and C^+ is a pseudo inverse.

3. Results and discussion:

For ferromagnetic films with simple cubic structure, Z_0=4, Z_1=1, Z_2=0 and $\Phi_0 = 9.0336$, $\Phi_1 = -0.3275$ [7, 8, 9]. All the data are given here for film films with three layers (N=3). Previously, the third order perturbed Heisenberg Hamiltonian with only the magnetic exchange energy, second order anisotropy, and the stress induced anisotropy terms has been solved by us. Here all the seven magnetic energy terms will be considered.

Figure 1 shows the 3-D plot of $\frac{E(\theta)}{\omega}$ versus angle and $\frac{K_s}{\omega}$. Magnetic easy directions are observed at $\frac{K_s}{\omega}$=11, 21, ----etc. Hard directions appear at $\frac{K_s}{\omega}$=7, 17, 27, -----etc. Two magnetic
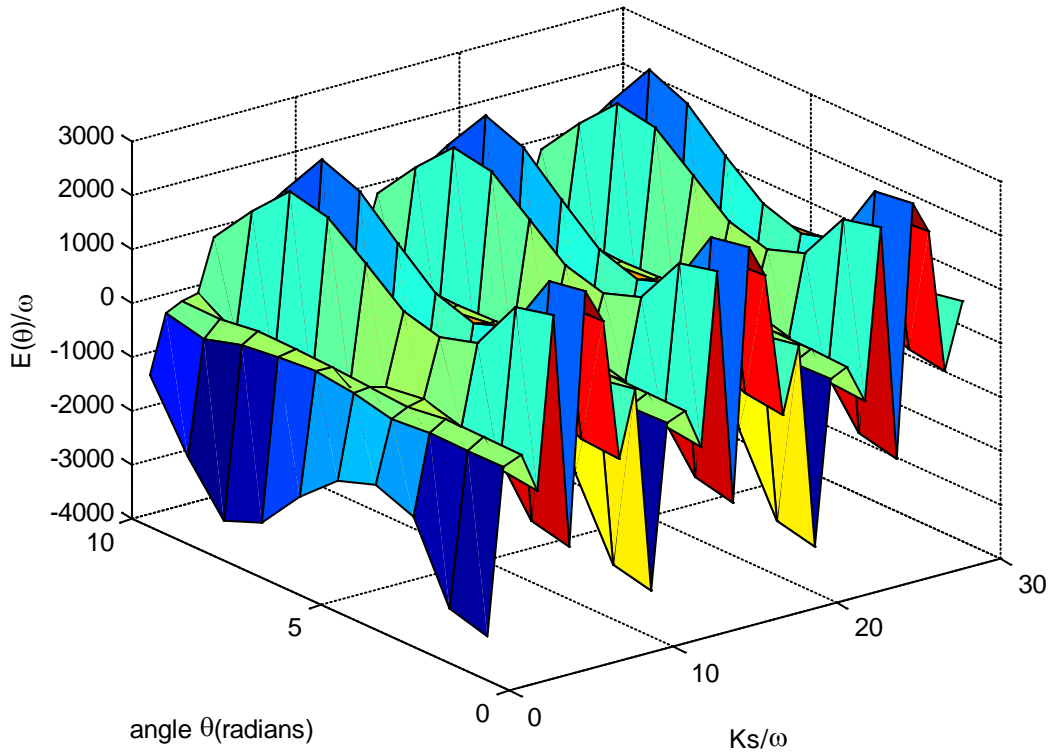
Figure 1: 3-D plot of $\dfrac{E(\theta)}{\omega}$ versus angle and $\dfrac{K_s}{\omega}$.

hard directions with different energies can be observed. Similarly two magnetic easy directions with different energies can be seen. The $\dfrac{K_s}{\omega}$ values at hard directions with higher energy and easy directions with lower energy are given here. Hard and easy directions can be observed at 8 and 4 radians, respectively. Other parameters were kept at $\dfrac{J}{\omega} = \dfrac{H_{in}}{\omega} = \dfrac{H_{out}}{\omega} = \dfrac{N_d}{\mu_0 \omega} = 10$, $\dfrac{D_m^{(2)}}{\omega} = 30$ and

$\dfrac{D_m^{(4)}}{\omega} = 20$ for this simulation. Previously 3-D plot of energy versus K_s and angle was plotted for sc ferromagnetic films using third order perturbed Heisenberg Hamiltonian with few terms only [24]. Compared to that graph, many peaks can be observed in this case due to the consideration of other terms. In addition, the shape of the graph was entirely different.

Figure 2 shows the 3-D plot of $\dfrac{E(\theta)}{\omega}$ versus angle and $\dfrac{H_{out}}{\omega}$. Here other parameters were kept at $\dfrac{J}{\omega} = \dfrac{H_{in}}{\omega} = \dfrac{K_s}{\omega} = \dfrac{N_d}{\mu_0 \omega} = 10$, $\dfrac{D_m^{(2)}}{\omega} = 30$ and $\dfrac{D_m^{(4)}}{\omega} = 20$ for this simulation. Magnetic easy directions can be observed at $\dfrac{H_{out}}{\omega} = 2, 7, 12,$ ---etc. Magnetic hard directions appear at $\dfrac{H_{out}}{\omega} = 1, 11,$ 21, ---etc. In addition to these major magnetic easy and hard directions, some minor easy and hard directions can be observed. Hard and easy directions of magnetizations appear at 4 and 5.57 radians, respectively. Angle between easy and hard directions is 90 degrees in this case.
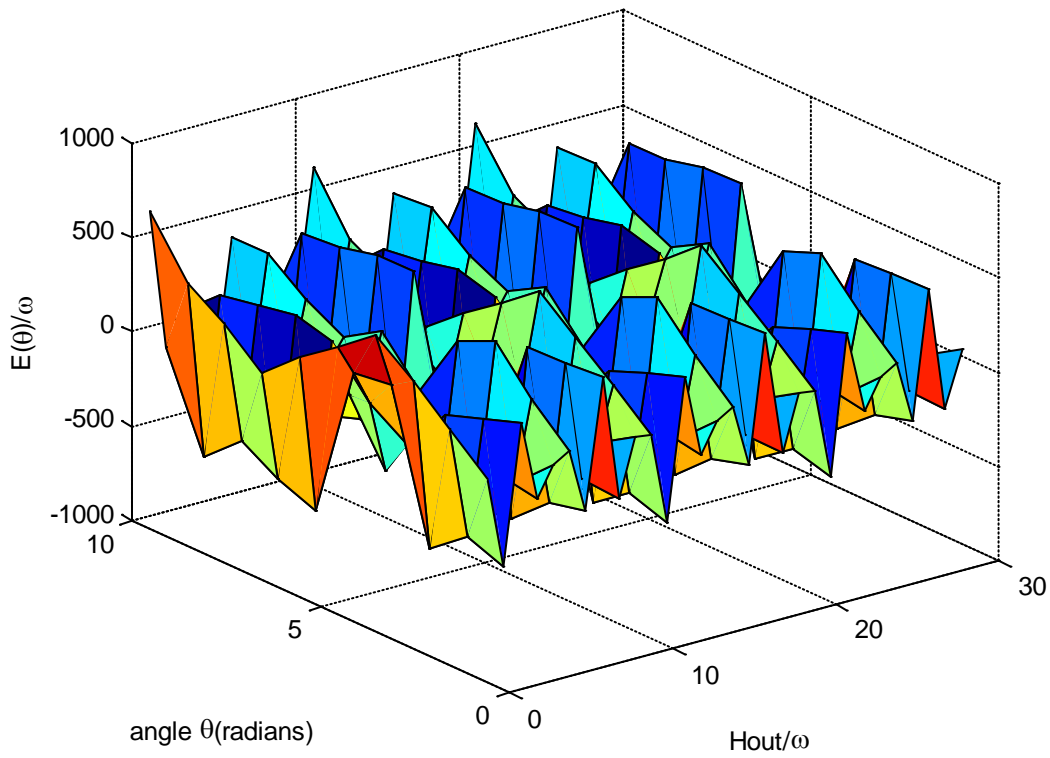
Figure 2: 3-D plot of $\dfrac{E(\theta)}{\omega}$ versus angle and $\dfrac{H_{out}}{\omega}$.

Figure 3 shows the 3-D plot of $\dfrac{E(\theta)}{\omega}$ versus angle and $\dfrac{N_d}{\mu_0\omega}$. Other parameters were kept at

$\dfrac{J}{\omega} = \dfrac{H_{in}}{\omega} = \dfrac{K_s}{\omega} = \dfrac{H_{out}}{\omega} = 10$, $\dfrac{D_m^{(2)}}{\omega} = 30$ and $\dfrac{D_m^{(4)}}{\omega} = 20$ for this simulation. Easy directions of

magnetization can be observed at $\dfrac{N_d}{\mu_0\omega} = 1$, 11, 21, ----etc. Hard directions of magnetization appear
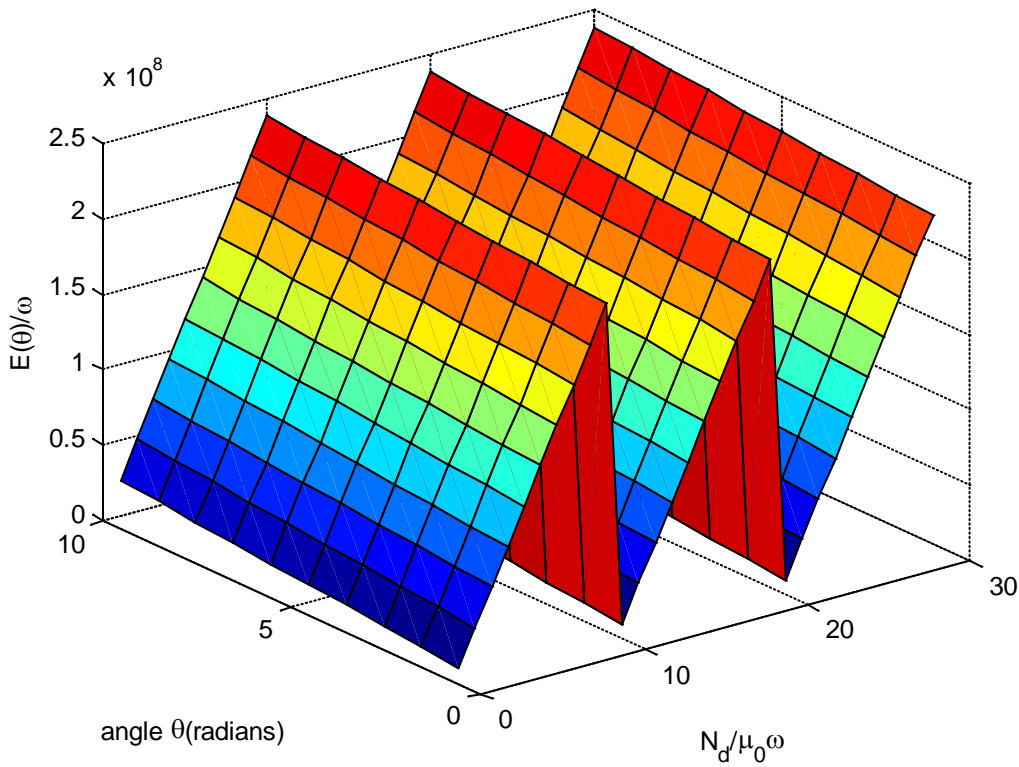
at $\dfrac{N_d}{\mu_0\omega} = 10$, 20, 30, ----etc.

Figure 3: 3-D plot of $\dfrac{E(\theta)}{\omega}$ versus angle and $\dfrac{N_d}{\mu_0 \omega}$.

Figure 4 indicates the 3-D plot of $\dfrac{E(\theta)}{\omega}$ versus angle and $\dfrac{J}{\omega}$. Other parameters were kept at $\dfrac{H_{in}}{\omega} = \dfrac{K_s}{\omega} = \dfrac{H_{out}}{\omega} = \dfrac{N_d}{\mu_0 \omega} = 10$, $\dfrac{D_m^{(2)}}{\omega} = 30$ and $\dfrac{D_m^{(4)}}{\omega} = 20$ in this case. Easy directions can be observed at $\dfrac{J}{\omega} = 10$, 20, 30, ----etc. Magnetic hard directions appear at $\dfrac{J}{\omega} = 1$, 11, 21, ----etc. Hard and easy directions of magnetizations appear at 3 and 6 radians, respectively.
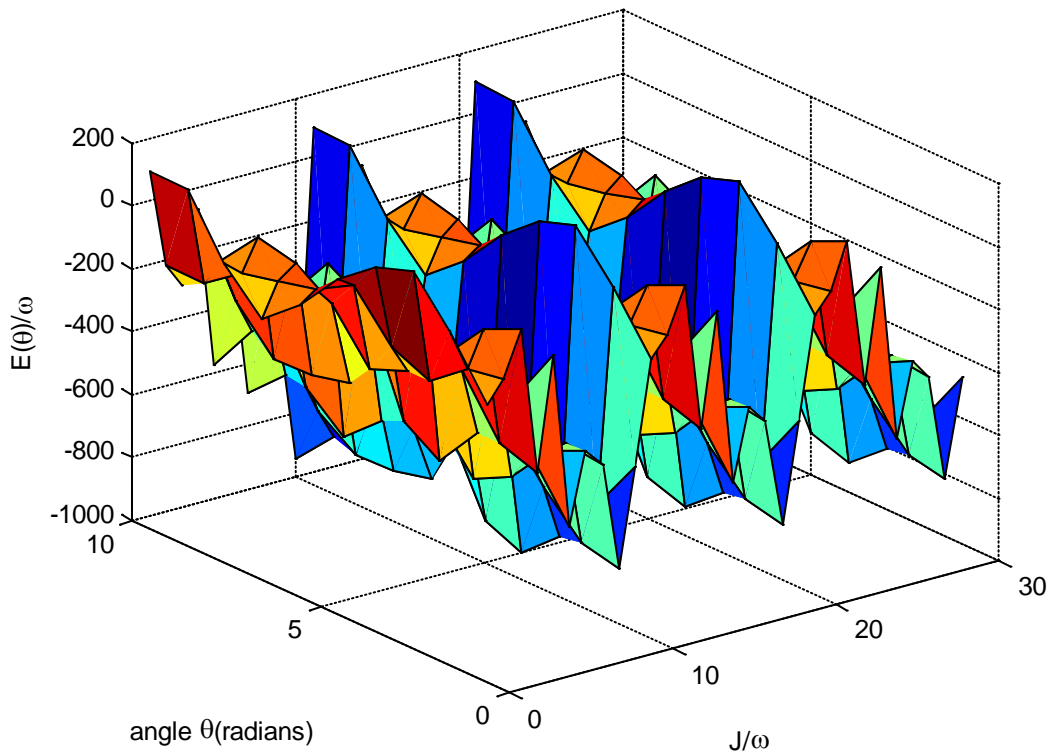
Figure 4: 3-D plot of $\dfrac{E(\theta)}{\omega}$ versus angle and $\dfrac{J}{\omega}$.

4. Conclusion:

Several magnetic easy and hard directions were found in the plots of $\dfrac{K_s}{\omega}$, $\dfrac{H_{out}}{\omega}$ and $\dfrac{J}{\omega}$.

However, only few peaks were found in the plot of $\dfrac{N_d}{\mu_0\omega}$. This may be related to the fact that

$\dfrac{N_d}{\mu_0\omega}$ contributes only a constant to the equation of total energy. According to figure 1, hard and

easy directions can be observed at 8 and 4 radians, respectively. According to figure 2, hard and easy directions of magnetizations appear at 4 and 5.57 radians, respectively. Easy directions of

magnetization can be observed at $\dfrac{N_d}{\mu_0\omega}$=1, 11, 21, ----etc and, hard directions of magnetization

appear at $\dfrac{N_d}{\mu_0\omega}$=10, 20, 30, ----etc. Hard and easy directions of magnetizations appear at 3 and 6

radians, respectively according to figure 4. The angle between easy and hard directions is 90 degrees only according to figure 2.

References:
1. Anna Radomska and Tadeusz Balcerzak, Central European Journal of Physics (2003), 1(1), 100.
2. James C. Cates and Chester Alexander Jr., Journal of Applied Physics (1994), 75, 6754.
3. A. Ernst, M. Lueders, W.M. Temmerman, Z. Szotek and G. Van der Laan, Journal of Physics: Condensed matter (2000), 12(26), 5599.
4. St Kovachev and J.M. Wesselinowa, Journal of Physics: Condensed matter (2009), 21(22), 225007.
5. D. Zhao, Feng Liu, D.L. Huber and M.G. Lagally, Journal of Applied Physics (2002), 91(5), 3150.
6. D. Spisak and J. Hafner, Journal of Magnetism and Magnetic Materials (2005), 286, 386.
7. K.D. Usadel and A. Hucht, Physical Review B (2002), 66, 024419.
8. A. Hucht and K.D. Usadel, Physical Review B (1997), 55, 12309-1.
9. A. Hucht and K.D. Usadel, Journal of Magnetism and Magnetic Materials (1999), 203(1), 88.
10. U. Nowak, IEEE transaction on magnetic (1995), 31(6-2), 4169.
11. M. Dantziger, B. Glinsmann, S. Scheffler, B. Zimmermann and P.J. Jensen, Physical Review B (2002), 66, 094416.
12. Shan-Ho Tsai, D.P. Landau and Thomas C. Schulthess, Journal of Applied Physics (2003), 93(10), 8612.
13. H. Hegde, P. Samarasekara and F.J. Cadieu, Journal of Applied Physics (1994), 75(10), 6640.
14. P. Samarasekara, Chinese Journal of Physics (2003), 41(1), 70.
15. P. Samarasekara, Chinese Journal of Physics (2002), 40(6), 631.
16. P. Samarasekara, Electronic Journal of Theoretical Physics (2006), 3(11), 71.
17. P. Samarasekara, Chinese Journal of Physics (2006), 44(5), 377.
18. P. Samarasekara, Electronic Journal of Theoretical Physics (2007), 4(15), 187.
19. P. Samarasekara and S.N.P. De Silva, Chinese Journal of Physics (2007), 45(2-I), 142.
20. P. Samarasekara, Inventi Rapid: Algorithm Journal (2011), 2(1), 1.
21. P. Samarasekara and William A. Mendoza, Georgian Electronic Scientific Journals: Physics (2011), 1(5), 15.
22. P. Samarasekara, Georgian electronic scientific journals: Physics (2010), 1(3): 46.
23. P. Samarasekara and Udara Saparamadu, Georgian electronic scientific journals: Physics (2013), 1(9), 10.
24. P. Samarasekara, Electronic Journal of Theoretical Physics (2010), 7(24), 197.

Article received: 2016-08-01